Investigating the Behavior of Sedimentary Mercury (Hg) During Burial-Related Thermal Maturation

A. O. Indraswari[1,2] , J. Frieling[1] , T. A. Mather[1] , A. J. Dickson[3] , H. C. Jenkyns[1] , and E. Idiz[1]

[1]Department of Earth Sciences, University of Oxford, Oxford, UK, [2]Geoscience Study Program, Faculty of Mathematics and Natural Sciences (FMIPA), Universitas Indonesia, Depok, Indonesia, [3]Centre of Climate, Ocean and Atmosphere, Department of Earth Sciences, Royal Holloway University of London, Surrey, UK

Abstract Understanding the behavior of mercury (Hg) in organic-rich sediments as they undergo thermal maturation is important, for example, because enrichment of Hg in sedimentary deposits has become a widely used proxy for volcanism from Large Igneous Provinces (LIPs). In this study, we evaluate the effects of such processes on sedimentary Hg concentrations by investigating a common stratigraphic interval in three drill cores with different levels of thermal maturity (immature, mature and post-mature) in Toarcian sediments (Posidonienschiefer Formation) from the Lower Saxony Basin, Germany. We present Hg concentrations, bulk organic geochemistry, and total sulfur data. Mercury concentrations in the mature and post-mature sediments are increased >2-fold relative to the immature material, which is greater than any potential differences in original Hg concentrations in the studied successions prior to burial. Organic-carbon and host-rock mass loss during thermal maturation may have concentrated Hg in the mature sediments to some extent, provided Hg is considered effectively immobile. The increased Hg, TOC-normalized Hg, and TS-normalized Hg are most likely linked to the "closed system" behavior of Hg in sedimentary basins and the relatively low temperatures (70–260°C) during maturation that resulted in limited Hg mobility. More speculatively, a certain degree of redistribution of Hg within the mature sediments is suggested by its enrichment in distinct stratigraphic levels. Regardless of the exact mechanisms at play, the elevated Hg concentrations in mature sediments amplify both Hg/TOC and Hg/TS, implying that thermal effects must be considered when using normalized Hg as a proxy for far-field volcanic activity.

Plain Language Summary This study examines how mercury (Hg) behaves in organic-rich sediments that undergo thermal maturation, which is crucial for using Hg concentrations as a proxy for paleo-volcanic activity. We analyzed three drill cores from the Lower Saxony Basin in Germany, each representing different stages of thermal maturity (immature, mature, and post-mature). We measured Hg concentrations, organic content, and sulfur levels in these sediments. We found that mature and post-mature sediments show more than double the Hg concentrations compared to immature sediments. This increase is likely due to the loss of organic matter and rock mass during maturation, which concentrates the remaining Hg. The relatively low temperatures (70–260°C) during maturation kept Hg from moving significantly, resulting in higher concentrations in mature sediments. There might be some redistribution of Hg within mature sediments, seen as enrichment in certain layers. Overall, the study highlights that thermal maturation effects must be accounted for when using Hg as a proxy for paleo-volcanic activity.

1. Introduction

Mercury (Hg) is a highly toxic metal. Thus, understanding its behavior in shallow- and deep-earth environments, and how it cycles through ecosystems, is of considerable importance (UN Environment, 2019). A major natural source of Hg in the environment is from volcanic exhalations (Pyle & Mather, 2003). Subsequent transport and deposition as dissolved or sorbed species is ultimately followed by removal into biomass in both terrestrial and aquatic settings (e.g., Fitzgerald & Lamborg, 2014; Grasby et al., 2019; Them et al., 2019). Consequently, mercury in the geological record is commonly associated with organic matter in marine, lacustrine, and terrestrial sediments (Fitzgerald & Lamborg, 2014; Grasby et al., 2019; Sanei et al., 2012). It is generally accepted that most Hg will be finally sequestered in sediments containing organic matter (OM) as OM-Hg complexes and associated sulfides. Indeed, field-data show that OM is a very effective scavenging ligand and likely the dominant carrier of Hg in the water column and sediments (Benoit et al., 2001; Outridge et al., 2007; Wallace, 1982).

1.1. Host Phases for Sedimentary Hg and Its Use as a Proxy for Paleo-Volcanic Activity

As volcanoes are amongst the largest natural sources of Hg in the atmosphere (Pyle & Mather, 2003), there has been much recent interest in the potential for their presence in sediments to serve as a proxy for large-scale volcanism, particularly in periods characterized by emplacement of large igneous provinces (LIPs) (Grasby et al., 2019; Percival et al., 2015, 2021; Pyle & Mather, 2003; Sanei et al., 2012). To detect anomalous Hg loading in sedimentary deposits, Hg concentrations are usually normalized with respect to total organic carbon (TOC) to correct for increases associated with larger amounts of organic matter (e.g., Grasby et al., 2019; Sanei et al., 2012). However, Hg can also be bound to sulfides and clay minerals, and in some environments, association with such geochemical species may complicate the usual relationship found between sedimentary OM and Hg (see e.g., Charbonnier & Föllmi, 2017; Percival et al., 2018; Sanei et al., 2012; Shen, Algeo, et al., 2019; Shen et al., 2020). Thus, several authors have argued that it is critical to examine the relationship of Hg not only with TOC but also with clay (Al) and total sulfur (e.g., Grasby et al., 2019; Shen et al., 2020). Moreover, OM source types (i.e., marine- vs. terrestrially derived OM) may also alter the Hg-OM relationship and thus may complicate the interpretation of deep-time sedimentary Hg records (Grasby et al., 2017; Them et al., 2019; Wang et al., 2018).

Fine-grained organic-rich sediments (typically shales and coals) commonly contain labile organic matter inherited from the original biomass (e.g., algal and vascular plant matter). Such sediments were often deposited under reducing conditions that enhanced the preservation of OM by hindering its degradation and remineralization (see e.g., Bohacs et al., 2020; Dembicki, 2022; Tissot & Welte, 1984). These deposits commonly are source rocks for petroleum as the labile organic matter can undergo transformation, converting to oil and gas as a result of burial and exposure to thermal stress (Dembicki, 2022).

1.2. The Presence of Hg in Hydrocarbon Reserves

Mercury, in various chemical forms, is commonly found in coals, petroleum and their combustion products in highly varying concentrations (Wilhelm & Bloom, 2000). For example, Hg concentrations range from 7 to 30,000 ppb in fuel oils (Mukherjee et al., 2009; Wilhelm, 2001). However, the presence of Hg in hydrocarbon fluids that are generated and expelled from such source rocks is still not well studied. In fact, there are divergent views as to whether or not the primary depositional environment and OM type is the main driver of Hg enrichment (Bryndzia et al., 2023; Li et al., 2019; Liu, 2013) or whether enhanced mercury concentrations in oil and gas deposits are mainly caused by secondary geological processes, such as interaction of hydrocarbon reservoirs with metal-rich hydrothermal fluids and formation waters (Filby, 1994) and adjacent volcanic rocks (Zettlitzer et al., 1997). High Hg concentrations have also been observed in hydrocarbon reservoirs associated with deep-faulted basement and mantle degassing (Liu et al., 2020). The intricate interplay between hydrocarbons and mercury (Hg) within a sedimentary basin is crucial to understand, as hydrocarbons have the potential to redistribute Hg across the basin, potentially disrupting the environmental-proxy relationship established by Hg distribution.

1.3. Effects of Thermal Maturation

Thermal maturation of labile sedimentary OM can occur due to increasing temperature with increasing burial depth, with average temperature gradients for sedimentary basins typically ranging between 20°C km^{-1} and 40°C km^{-1} (Gluyas & Swarbrick, 2021). As sediments become buried, the organic matter initially undergoes diagenesis, which eliminates functional groups and moieties that are primarily oxygen- and nitrogen-containing, resulting in a resistant macromolecular residue (kerogen) and sulfur (Tissot & Welte, 1984). This kerogen can be further broken down into lower molecular weight hydrocarbon species, such as oil and gas, through the process of thermal cracking (Dembicki, 2022; Peters et al., 2005; Tissot & Welte, 1984). As the kerogen becomes more thermally "mature" it progresses through the stages of oil and gas generation and, depending on the type of kerogen, potentially loses up to 60% of its organic-matter mass due to secondary migration of the generated products away from the host rock (Dembicki, 2022; Lewan et al., 1979; Raiswell & Berner, 1987; Tissot & Welte, 1984). With sufficient burial and extended exposure to high basinal temperatures, the original kerogen ultimately ends up as a carbon-rich graphitic residue, having lost most of its labile organic matter as expelled H-rich hydrocarbon species.

Thermal maturation may play a key role in altering the geochemical signature of metals in sediments (e.g., Mo, V, and Ni) due to the close association of these geochemical species with sedimentary OM and the transformations that it undergoes (Chappaz et al., 2014; Dahl et al., 2017; Lewan & Maynard, 1982). For example, thermal

maturation has been shown to lead to progressive enrichment in both the concentration of metals and their TOC-normalized values in sedimentary rocks for Mo, Zn, U and Cd (Ardakani et al., 2020; Dickson et al., 2020, 2022). Such increases can be attributed to the progressive loss of mass caused by the migration of bitumen formed during thermal maturation and only minor partitioning of metals into mobilized organic fluid phases, rendering them effectively immobile in sedimentary strata (Dickson et al., 2020, 2022). Compared to these metals, we do not know how Hg might be expected to transfer into a hydrocarbon fluid phase, especially because data on processes influencing trace elements in hydrocarbons are limited (Bryndzia et al., 2023). The accompanying generation of H_2O, CO_2, and H_2S from both the organic and inorganic phases in such rocks might also play a role in causing additional loss of mass (Abarghani et al., 2020; Dickson et al., 2020). However, it is difficult to directly measure metals bound to kerogen since the primary method to isolate this organic component is by digesting the mineral matrix using strong acids such as HF and HCl, which can also leach metals from the kerogen itself. Consequently, the mechanistic behavior of metals, including Hg, in OM-rich sediments as they undergo thermal maturation, is still not well understood.

1.4. Behavior of Hg During Maturation

Previous studies have investigated various factors influencing sedimentary Hg concentrations (Grasby et al., 2019; Shen et al., 2020), including the effects of contact metamorphism associated with igneous intrusions (Svensen et al., 2023), and by the use of artificial maturation experiments in the laboratory (Chen et al., 2022; Li et al., 2016; Liu et al., 2022). Mass-independent Hg-isotope fractionation signatures are commonly used to determine original depositional pathways of Hg in sedimentary records (e.g., Dal Corso et al., 2020; Thibodeau et al., 2016). Recent studies by Chen et al. (2022) and Liu et al. (2022) suggested that mass-dependent isotope fractionation may occur during heating, but mass-independent fractionation signatures appear to be mostly retained.

Despite efforts to study the behavior of Hg in experimental settings, the behavior of Hg in sediments exposed to gradual maturation due to burial in sedimentary basins has not been systematically tested using natural samples. Conditions imposed on sediments in existing (experimental) maturation studies may differ from sediments matured through burial in two critical aspects that may influence Hg mobility. First, the conditions of deeply buried sediments are difficult to replicate in laboratory experiments, for example, near-impermeable (clay-rich) strata may behave as a closed system, which could limit the mobility of hydrocarbons and Hg. Second, the temperatures experienced by the sediments in most maturation experiments (maximum temperature of 610°C in Liu et al. (2022) and 700°C in Chen et al. (2022)) as well as sediments sampled from the thermal aureoles of igneous intrusions might be much higher than those experienced during natural burial conditions (60–225°C; Tissot & Welte, 1984). These considerations require critical attention because most sedimentary Hg species (OM-bound Hg, pyrite and metacinnabar) can be mobilized at temperatures known to be relevant for post-depositional sediment alteration and resulting oil and gas generation (e.g., Liu et al., 2022; Rumayor et al., 2013; Saniewska & Bełdowska, 2017). Indeed, thermal desorption studies and laboratory maturation experiments also showed release of several relevant Hg-species even with short-term exposure to low (~150°C) temperatures (Reis et al., 2012, 2015; Saniewska & Bełdowska, 2017). Moreover, Hg is clearly enriched in some but surprisingly low in other hydrocarbon fluids (e.g., Mukherjee et al., 2009; Wilhelm, 2001), which might reflect variable release and mobility, which is a function of the original concentration of Hg in the source rocks and its host phase. Extrapolating these observations over geological timescales, we may therefore hypothesize that mature sedimentary strata should contain ubiquitously low Hg concentrations. The extensive geological records of Hg, including those in mature sediments, show this is clearly not the case. For example, the outcrop section of the Lower Jurassic Fernie Formation is overmature ($T_{max} > 500°C$) (Them et al., 2017), albeit enriched in Hg (maximum concentration of 232 ppb), which was identified as a signal of Karoo-Ferrar LIP volcanism (Them et al., 2019). The high Hg concentrations found in thermally mature sections suggests that additional processes must play a role in shaping the Hg records of buried strata that were exposed to burial-related maturation, and that these effects are not captured in current experiments (e.g., Chen et al., 2022; Liu et al., 2022).

Unlike most metals, there is evidence from thermal desorption analyses on chemical species of Hg that sediments exposed to temperatures during the burial typical of evolving sedimentary basins could mobilize some Hg compounds. Slow release of many Hg-species during exposure to moderate heating over geological timescales may lead to much more pronounced Hg loss from sedimentary strata, in line with sediments affected by much higher temperatures (e.g., Chen et al., 2022; Liu et al., 2022). While simultaneous mass loss of the host rock may
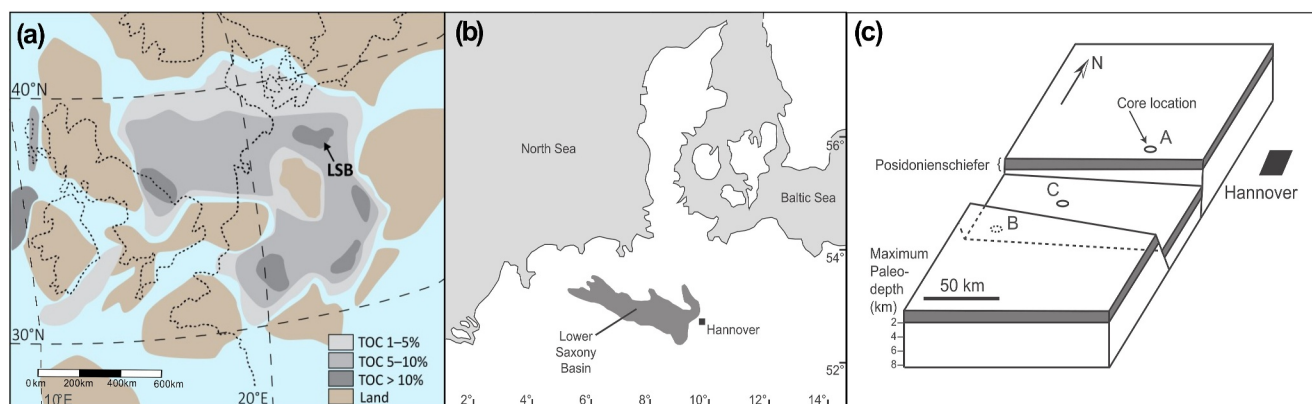
Figure 1. (a) Location of the Lower Saxony Basin (LSB) in the Early Jurassic epicontinental seaway of northern Europe (ca. 182 Ma) (after Dickson et al., 2022). Modern shorelines are shown as dashed lines. TOC—total organic carbon—contents in wt% are indicated by gray shading. (b) Map of the study area (modified from Kockel et al., 1994 and after Hooker et al., 2020). (c) Schematic block diagram showing locations of cores in this study, synthesized from Baldschun et al. (1996). Shaded layer shows approximate maximum paleodepth of the top of the Posidonienschiefer (after Hooker et al., 2020).

offset some of the Hg release in a similar fashion to other (immobile) elements (see also §1.3), the majority of records showing high Hg concentrations in mature sediments suggest that its near-complete loss is very unlikely to have occurred (e.g., Bian et al., 2022; Grasby et al., 2019; Them et al., 2019). The combined effects on Hg of prolonged exposure to the pressure and temperature regimes that typically exist during maturation therefore remain elusive.

Our study explores the influence of thermal maturation on sedimentary Hg using three cores (A, B and C) covering a wide range of thermal maturities from Toarcian sediments of the Lower Saxony Basin, Germany. By investigating Hg concentrations, bulk OM characteristics and total sulfur (TS) concentrations in a stratigraphically constrained interval from a single basin, we examined the role of thermal maturation as a key factor in post-depositional Hg mobility in sediments. We focus on the Posidonia Shale or Posidonienschiefer Formation (hereafter referred to simply as the Posidonienschiefer).

2. Geological Setting and Samples

The Lower Saxony Basin (LSB) is located in northwestern Germany (Figure 1) and is a 300-km long and 65-km wide E–W-oriented basin formed during the breakup of the supercontinent Pangea through extension and subsidence (Betz et al., 1987; Brink et al., 1992; Bruns et al., 2013). The Lower Toarcian Posidonienschiefer (also known as Lias Epsilon Formation) is a well-studied, distinct organic-rich unit preserved in the LSB, bracketed by marls and carbonate-rich units of the overlying Lias Delta Formation and underlying Lias Zeta Formation (Littke et al., 1991). It is a prolific source rock for petroleum produced from several significant fields within the LSB (Kockel et al., 1994).

Deposition of the Posidonienschiefer within a restricted basin with high productivity and highly reducing conditions led to preservation of algal and bacterial biomass over a significant stratigraphic interval, resulting in 20–40 m of sediments with high amounts of total organic carbon (TOC) and elevated hydrogen indices (HI) (Celestino, 2019). A stratigraphically related organic-rich interval was also deposited and preserved in various other fault-bound basins in northwest Europe and elsewhere (Jenkyns, 1985, 1988; Littke et al., 1988, 1991; Rullkötter et al., 1988; Schmid-Röhl et al., 2002; Schwark & Frimmel, 2004). Extensive basin-wide sulfidic conditions and persistent euxinia in the water column during deposition, including indicators of free H_2S in the photic zone, is evidenced by the presence of aryl isoprenoids and other diagnostic carotenoids reported in the Posidonienschiefer from the LSB (Blumenberg et al., 2019) and from other NW European basins (Celestino, 2019; French et al., 2014; Schwark & Frimmel, 2004; Song et al., 2017). Further evidence of such basin-wide highly reducing and sulfidic conditions is found in the elevated concentrations and isotope ratios of redox-sensitive metals (Mo, Cd, U, Zn) and Fe-speciation data reported by Celestino (2019) and Dickson et al. (2020, 2022) in the Posidonienschiefer from samples from the LSB as well as from other basins in Europe (Montero-Serrano et al., 2015; Röhl et al., 2001).

Since its deposition in the Early Jurassic, the Posidonienschiefer has been buried to varying depths due to differential subsidence within the fault bounded LSB, followed by basin inversion during the Paleogene (Betz et al., 1987). As a result, the thermal maturity of the OM contained within the Posidonienschiefer varies significantly over relatively short horizontal distances of tens of kilometers. This variation in maturity, combined with a correlatable interval with very similar organofacies and depositional environmental conditions, makes the Posidonienschiefer in the LSB an ideal candidate for testing the impact of thermal maturation on the concentration of metals such as Hg in organic-rich sedimentary rocks.

Three cores (A, B and C) containing approximately 30-m-thick stratigraphically equivalent sections of the Posidonienschiefer as well as sections of the Lias Delta Formation and Lias Zeta Formation were studied from different parts of the LSB (Figure 1). These cores have been the focus of a variety of previous studies, including the impact of maturity on the stable-isotope compositions and concentrations of the redox-sensitive and/or chalcophilic trace metals Mo, Zn, Cd and U (Dickson et al., 2020, 2022), and for chemostratigraphy and basic organic and inorganic geochemical parameters (Celestino, 2019; Celestino et al., *submitted*). Core-to-core correlation of the Posidonienschiefer interval that post-dates the sediments recording the Toarcian Ocean Anoxic Event (T-OAE, see Celestino, 2019; Celestino et al., *submitted*) was achieved using distinct basin-wide chemostratigraphic trends in the TOC and trace-metal records. We utilize the interval of the Posidonienschiefer that was deposited after the T-OAE (Jenkyns, 2010) to avoid the Hg-cycle perturbation that characterizes this major paleoceanographic event (Celestino, 2019; Celestino et al., *submitted*; Fantasia et al., 2018; Percival et al., 2015; Them et al., 2019).

The thermal maturity of each core was previously established by organic petrography yielding vitrinite reflectance (%Ro) measurements of 0.5%–0.7%, 1.5%, and 3.5% for cores A (immature), B (mature), and C (post-mature), respectively (Gorbanenko & Ligouis, 2014, 2015). Cores B and C represent an upper end-member with extremely high maturity, whereas core A represents maturity levels more commonly used in Hg studies and encompasses the hydrocarbon formation window. The present-day depths and subsurface temperatures for the three cores do not represent peak burial and temperatures experienced in the past by the cores due to the significant inversion history of the LSB. The maximum burial depth and exposure temperature data were obtained from a basin modeling study by Bruns et al. (2013), which used a calculated average temperature gradient during maximum subsidence in the central part of the LSB of ∼47°C/km (Senglaub et al., 2006), and determined maximum burial depths of ∼1,500, ∼4,300, and ∼5,600 m, respectively, for cores A, B, and C. The calculated peak burial temperatures for the cores are 70°C (core A), 200°C (core B), and 260°C (core C) and were acquired by multiplying the maximum burial depth with the basin temperature gradient.

Two key factors postulated to have significant impact on the sequestration and concentrations of Hg (and other metals) in sedimentary systems are redox conditions and type of organic matter (see Grasby et al., 2019; Frieling et al., 2023 and references therein). Trace-metal, organic geochemical and organic petrographic data from previous studies on these 3 cores (Celestino, 2019; Dickson et al., 2020, 2022; Gorbanenko & Ligouis, 2014, 2015) show persistent euxinic conditions and input of primarily marine-derived organic matter throughout the deposition of the Posidonienschiefer in the LSB. Consequently, these two variables were not considered a significant factor in our study of long-term maturation effects on Hg concentrations in the LSB cores (see discussion section below, for a more detailed evaluation of these and other variables).

3. Methods

A total of 301 sediment samples from the Posidonienschiefer, 217 for core A, 49 for core B, and 35 for core C (Table S1 in Supporting Information S1), were powdered and analyzed for Hg concentrations using a Lumex RA-915 Portable Mercury Analyzer coupled to a PYRO-915+ pyrolysis unit at the University of Oxford (Bin et al., 2001). Powdered samples of between 50 and 100 mg were introduced into a sample boat, heated to >700°C and left for up to 120 s to fully volatilize the Hg present. The instrument was calibrated before each run using NIST-SRM2587 (National Institute of Standards and Technology—Standard Reference Material: Trace Elements in Soil Containing Lead from Paint) with an Hg concentration of 290 ± 9 ppb. The same standard was run every 10 samples to correct instrument drift. We calculated an external reproducibility of ±8.7% based on the repeat standard measurements (1 standard deviation (S.D.), $n = 199$).

Six different samples of Lower Saxony Basin oils sourced from the Posidonienschiefer (Stock & Littke, 2016) were obtained from the Oil Museum in Germany. These fluids were analyzed for Hg concentrations using the

same instrument (Lumex RA-915) used for sediments. An amount (about 0.2 g) of activated charcoal was spread on the inner surface of a quartz boat of the Lumex pyrolyzer. Subsequently, a known mass of oil was added onto the charcoal bed and analyzed. Each sample was measured 5 times. The instrument was calibrated before each run using the same paint standard as the sediments above as well as an additional oil standard NIST-SRM2778 (National Institute of Standards and Technology—Standard Reference Material: Mercury in Crude Oil) with a Hg concentration of 39 ppb. The standards were run every seven samples to correct for instrument drift. We calculated an external reproducibility of ±3.64% (1 S.D., $n = 12$) for the repeat standard measurements of Paint, and ±5.88% ($n = 5$) for the oil standard. Hydrogen and Oxygen indices (HI, OI) and TOC data from all three cores have been published previously in Celestino (2019), Hooker et al. (2020), and Dickson et al. (2020, 2022). An additional 39 new samples (15 for core A, 21 for core B, and 3 for core C) (annotated in Data Set S1) were analyzed with a Rock-Eval 6, following the methods in Behar et al. (2001), at the University of Oxford. The in-house standard SAB134 (Blue Lias organic-rich marl, 2.74% TOC) was measured every 8 to 10 samples. The standard deviation of the in-house standard (SAB134) was ~0.03% TOC (1 S.D.).

Analyses of total sedimentary sulfur (%TS) were undertaken on 155 samples (57 for core A, 50 for core B, and 48 for core C). The samples were selected to cover the full range of Hg concentrations observed within the stratigraphic intervals of interest to allow the relationship of Hg and S to be quantified. An aliquot of each sample was wrapped in a tin capsule and combusted using an Elemental Cube Elemental Analyzer Vario El III at the Department of Earth Sciences, Royal Holloway University of London. A sulfanilamide reference standard (18.62% S) was analyzed at the start and end of each run and between every 10 samples to monitor instrument drift. Within-run reproducibility calculated from the in-house shale standards (1.24% S) run as unknowns was ±0.12% S (1 S.D., $n = 12$).

4. Results

4.1. Bulk Sediment Chemistry and Maturity (TOC, TS, HI and OI)

The organic-rich intervals of the Posidonienschiefer (PS) in the three cores used in this study are all stratigraphically above the sections that record the negative carbon-isotope excursion characteristic of the T-OAE (Jenkyns, 2010; Celestino, 2019; Celestino et al., *submitted*). TOC values in all the cores are relatively elevated in the Posidonienschiefer interval, ranging between ~5%–14%. The average TOC values in all the cores are within a comparable range (8.3%–9.8%) despite the differences in maturities, and show a modest increase from core A to core B and from core B to core C (Table 1). TOC variability within the Posidonienschiefer section of each core is greater than the variability between the cores. The most notable trend up-section is seen in the immature core A, where there is a decrease from ~14% at the base to a minimum of ~5% in the central section of the Posidonienschiefer before increasing again to ~12% at the top. Hydrogen Index values for the same section in core A are rather high (600–750 mg HC/gTOC), and show little variation, despite the changes in TOC concentrations (Figure 2). Oxygen Index values are low throughout the section, generally below 10 mg CO_2/g TOC. By contrast, in cores B and C, the HI values throughout the Posidonienschiefer are near 0 (Figures 3 and 4), in line with their relatively high maturity and negligible to no remaining S2 or hydrocarbon generative potential.

Rock-Eval-determined T_{max} values are around 432–440°C for core A and attest to the immature (onset oil window) stage of conversion of the kerogen, in keeping with the measured vitrinite reflectance (%Ro) data (~0.5%–0.7%: Gorbanenko & Ligouis, 2014, 2015). The calculated %Ro equivalents from the T_{max} values (Evenick, 2021) of the immature core A are also in this range. In cores B and C, where the Rock-Eval S2 peak was too low for accurate T_{max} assessment, we relied on petrographically determined %Ro of 1.5% and 3.5%, respectively, for these two cores following Gorbanenko and Ligouis (2014, 2015). In terms of kerogen conversion and hydrocarbon generation, core A would be considered immature/onset of generation, core B is in the early dry gas window and core C is post-mature.

Total sulfur (TS) concentrations range from ~2% to 4.5% for the immature core A, and ~2%–5.5% for the mature to post-mature cores B, and C through the Posidonienschiefer (Figures 2–4). These ranges are comparable to data from previous organic geochemical studies of the Posidonienschiefer (e.g., French et al., 2014; Littke et al., 1991; Song et al., 2017) as well as organic petrography (Gorbanenko & Ligouis, 2014, 2015), which identified abundant (framboidal) pyrite and established that both the iron sulfide and organic matter are the primary hosts for the sulfur. Cores B and C show subtle but somewhat higher %TS values in the upper part of the section compared to the lower halves, while the range remains fairly constant for the whole section in core A.

Table 1

TOC, Hg, TS, HI, OI, and Trace-Metal Data for Cores A, B, and C From the Posidonienschiefer

		Core		
		A	B	C
Hg (ppb)	Mean	85.88	209.49	234.37
	Std. Dev.	21.76	76.77	67.39
TOC (%)	Mean	9.81	8.33	9.40
	Std. Dev.	2.21	2.00	1.82
TS (%)	Mean	3.32	3.61	3.64
	Std. Dev.	1.26	0.81	0.98
Hg/TOC (ppb/%)	Mean	9.08	25.13	25.72
	Std. Dev.	2.08	10.35	7.81
Hg/TS (ppb/%)	Mean	27.19	56.07	65.70
	Std. Dev.	7.50	16.63	12.98
Hydrogen Index[+] (mgHC/gTOC)	Mean	690	1	3
	Std. Dev.	36	1	3
Oxygen Index[+] (mgCO$_2$/gTOC)	Mean	6	11	12
	Std. Dev.	2	2	2
Cd* (ppm)	Mean	1.7		1.8
	Std. Dev.	1.1		0.6
Zn* (ppm)	Mean	178		217
	Std. Dev.	97		80
U* (ppm)	Mean	5.7		16.1
	Std. Dev.	2.4		11.8
Mo* (ppm)	Mean	70.45		101.9
	Std. Dev.	39.9		52.3

Note. Symbols [+] indicate data from Hooker et al. (2020) and * from Dickson et al. (2022).

4.2. Sedimentary Hg, Hg/TOC and Hg/TS Analyses

Within the Posidonienschiefer interval of the three cores, Hg concentrations fluctuate between 32 and 433 ppb, which are generally elevated above the typical mean values of Hg found in sedimentary rocks (62.4 ppb from the compilation in Grasby et al., 2019). In the correlated Posidonienschiefer intervals of cores A, B, and C, the ranges of Hg concentrations are 53–154 ppb (Figure 2), 28–397 ppb (Figure 3) and 32–433 ppb (Figure 4), respectively. The mean Hg concentration increases from 85 ppb (core A) to 203 ppb (B) and 225 ppb (C) (Table 1, Figure 5). Cores B and C have, on average, ~2.3–2.6-fold higher Hg than core A. Notably, the Hg concentrations in cores B and C show larger variability than core A and have clear maxima in the central and upper part of the core before decreasing again toward the top of the Posidonienschiefer (Figure 6). In cores B and C, Hg concentrations show remarkably similar patterns (Figure 6) with close correlation in the trends (peaks and troughs) between the two cores. In both the B and C cores, overall Hg concentrations are higher in the upper half of the section compared to the lower. This trend in Hg mimics the subtle differences in %TS (Figures 2–4) between the upper and lower halves of cores B and C noted in the previous section (§4.1).

Hg/TOC values in core A are in the range of 5–15 ppb/TOC%, 10–56 ppb/TOC% in core B, and 12–45 ppb/TOC% in core C. Hg/TOC ratios in core A vary over a narrow range around an average of ~10 ppb/TOC% throughout the Posidonienschiefer (Figure 2) whereas, in cores B and C, these values are overall higher and show significantly more variation in ranges (Figures 2–4). As with the Hg and TS concentrations and TOC/TS values, the Hg/TOC ratios in cores B and C (Figure 6) again have persistently higher values in the upper halves of the section compared to the lower.

The Hg/TS ratio in core A is relatively constant throughout the organic-rich Posidonienschiefer section (~20–40 ppb/TS%), while cores B and C have higher ratios (~38–90 ppb/TS% and ~42–90 ppb/TS%, respectively) and show more variability (Table 1 and Figures 5 and 6). Cores B and C have higher Hg/TS ratios in the upper half of the sections, with the former showing a decrease in the uppermost part (Figure 6). Overall, as with the Hg concentrations, the Hg/TS profiles for core B and C are quite similar in their changes up-section.

The Hg versus TOC shows a weak correlation ($R^2 = 0.395$) in core A and essentially none in cores B and C ($R^2 = 0.065$ and 0.032, respectively) (Table S2, Figure S2 in Supporting Information S1). Compared to Hg-TOC, Hg correlates only slightly better with TS for core B ($R^2 = 0.139, 0.363, 0.010$, for core A, B, C, respectively) (see Table S2 and Figure S2 in Supporting Information S1). There is a weak general trend of higher Hg with higher TS when the data from all three cores are taken together, with the higher maturity ones showing the most elevated values of Hg and TS (Figure S2 in Supporting Information S1). However, individual correlations between Hg, TOC and TS each explain less than 50% ($R^2 < 0.5$) of the observed variance, likely signaling that Hg is hosted by both TOC and sulfide phases and/or that neither strongly controls Hg variability. This pattern is expected because, for high-TOC and high-TS sediments, the Hg supply is often limiting (e.g., Fendley et al., 2024; Frieling et al., 2023; Schuster et al., 2018).

4.3. Hg Analyses of Oils

The results of Hg measurements in LSB oils are shown in Table 2. The mean concentration of Hg in Posidonienschiefer-derived oils is 3.4 ± 1.1 ppb (1 S.D.), which is at the lower end of the range of Hg reported in fuel oils (7–30,000 ppb; Wilhelm & Bloom, 2000). The amount of Hg found in produced oils is also significantly lower than the Hg concentration in the sediments, both mature and immature.
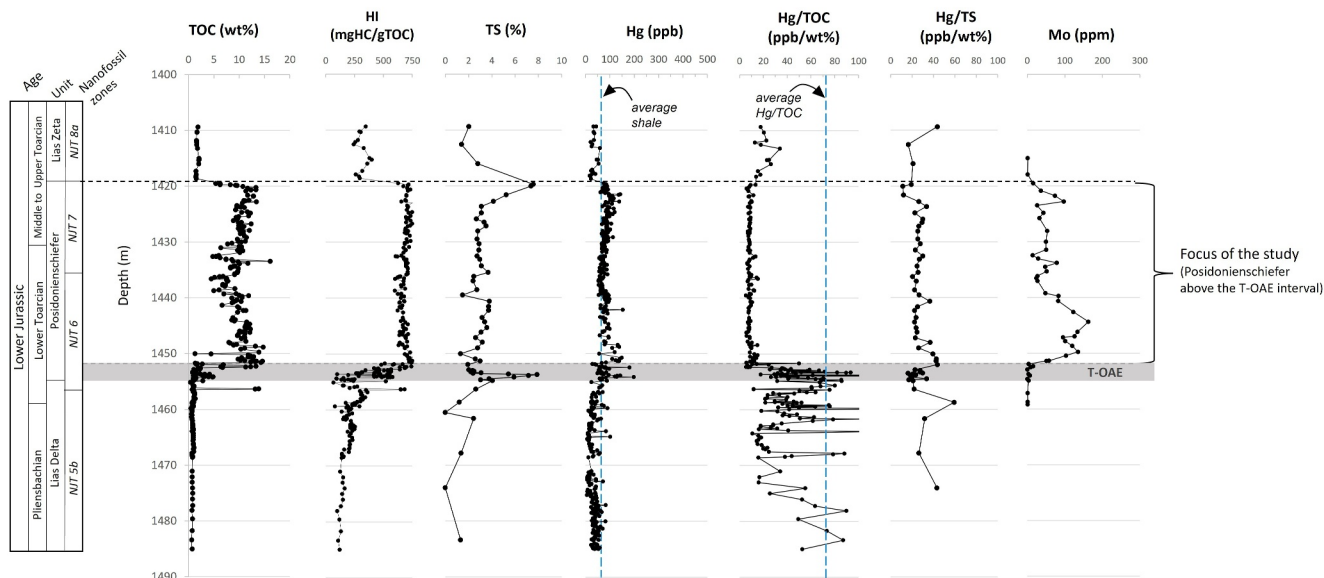
Figure 2. Stratigraphic log of the studied core A (immature, vitrinite reflectance, %Ro ~0.5%–0.7%) showing the total organic carbon (TOC), hydrogen index (HI), total sulfur (TS), Hg concentration, Hg normalized by TOC, Hg normalized by TS, and Mo concentration. Dashed lines showing average Hg concentration (62.4 ppb) and Hg/TOC (71.9 ppb/%) in shale from Grasby et al. (2019).
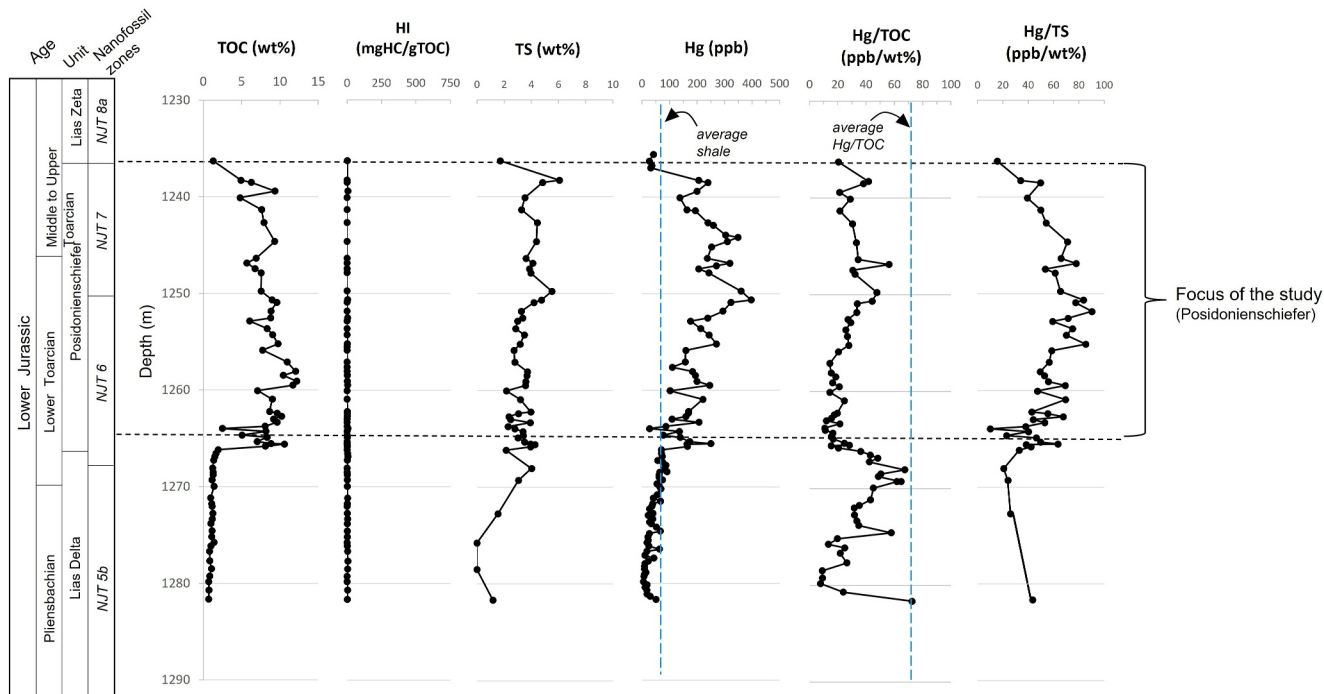
Figure 3. Stratigraphic log of the studied core B (mature, vitrinite reflectance, %Ro ~1.5) showing total organic carbon (TOC), hydrogen index (HI), total sulfur (TS), Hg concentration, Hg normalized by TOC, and Hg normalized by TS. Dashed lines showing average Hg concentration (62.4 ppb) and Hg/TOC (71.9 ppb/%) in shale from Grasby et al. (2019).

Figure 4. Stratigraphic log of the studied core C (post-mature, vitrinite reflectance, %Ro ~3.5) showing total organic carbon (TOC), hydrogen index (HI), total sulfur (TS), Hg concentration, Hg normalized by TOC, Hg normalized by TS, and Mo concentration. Dashed lines showing average Hg concentration (62.4 ppb) and Hg/TOC (71.9 ppb/%) in shale from Grasby et al. (2019).
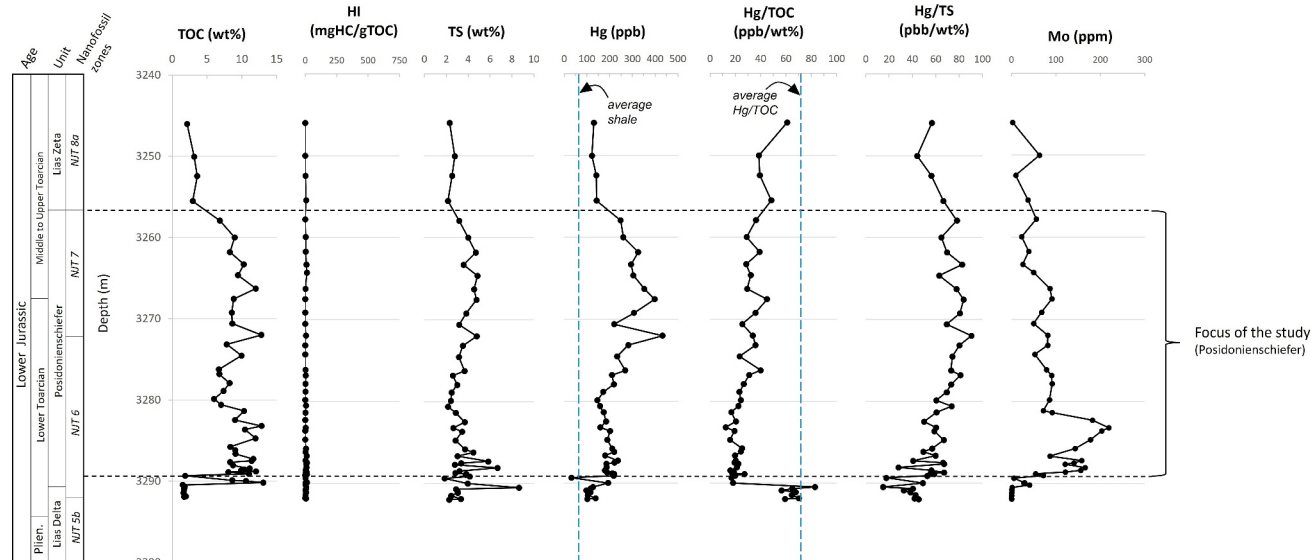
5. Discussion

5.1. Mercury Enrichment: Differences in OM Type and Original Depositional Environmental Conditions Between Cores?

In all three cores in our study, Hg concentrations in the organic-rich section of the Posidonienschiefer are higher than in the underlying Lias Delta and the overlying Upper Toarcian unit (Lias Zeta) (Figures 2–4). Increased Hg concentrations are coincident with the much higher TOC (measured and calculated original values) in the Posidonienschiefer and are marked by a change from the marls and carbonate-dominated lithologies stratigraphically above and below, differences that reflect very pronounced changes in depositional redox and sedimentary conditions (Dickson et al., 2022) as well as type and preservation of organic matter.

Differences in the original organic-matter concentration of the cores are evident, given that the mature and post-mature cores B and C have residual TOC values that are still in the same range as the immature core A, despite having undergone significant conversion of labile organic matter into hydrocarbons. Reconstructing original TOC for these two mature/post-mature cores using the method of Jarvie (2012) yields calculated original TOCs in cores B and C before thermal maturation of around ~16% and ~19%, respectively, which is significantly higher than the average TOC value in core A (~10%). This pattern of higher initial OM concentration in cores B and C could be
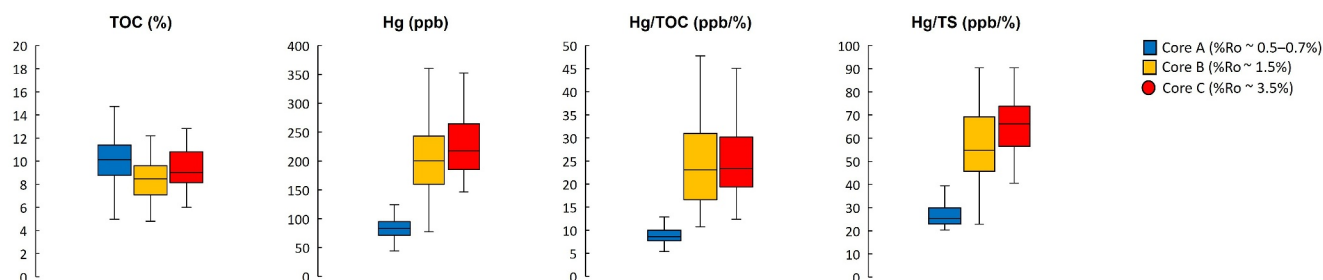
Figure 5. Differences between cores A, B and C in the mean (horizontal lines in the box), interquartile range (boxes) and data within 1.5 interquartile range (black lines with bar ends) of TOC (%), Hg (ppb), Hg/TOC (ppb/%), and Hg/TS (ppb/%) in the Posidonienschiefer.
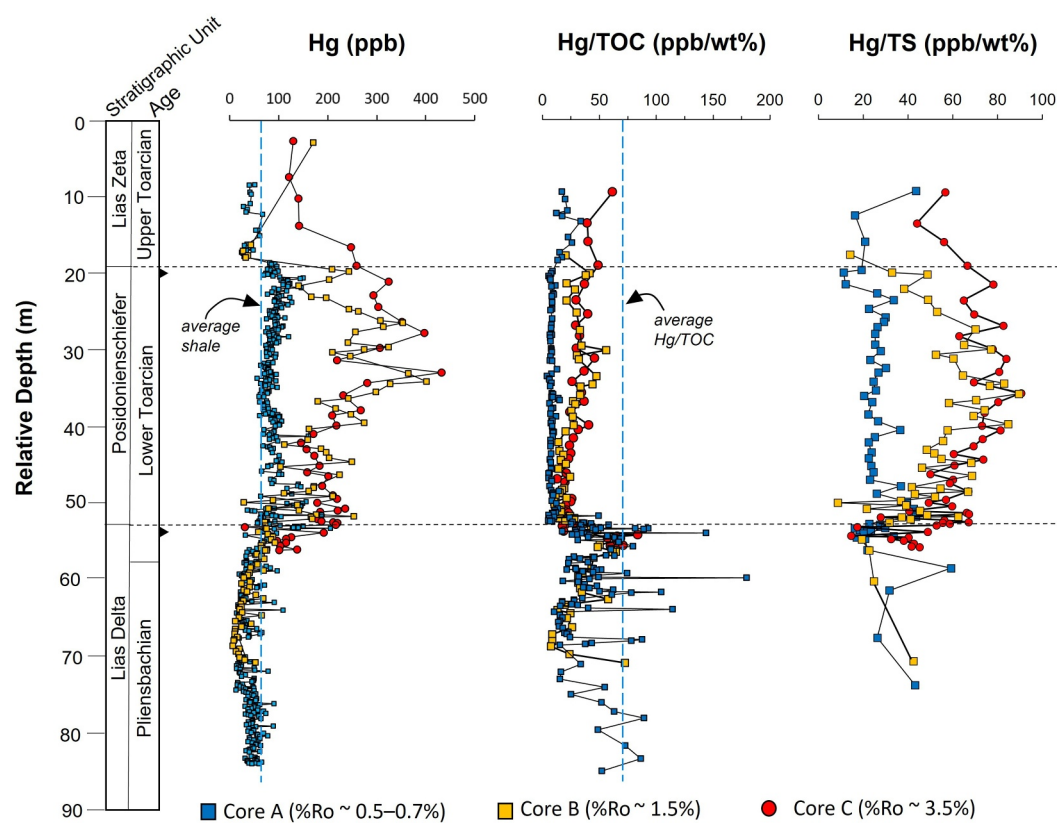
Figure 6. Hg concentrations, Hg/TOC, and Hg/TS in cores A, B, and C. Hg concentrations in cores B and C reached a maximum amount of ∼400 ppb at a relative depth of 34 m, up to 4 times the Hg concentrations in core A at the same depth. The Hg/TOC and Hg/TS ratios in core A diverge from those for cores B and C around a relative depth of ∼50 m, with values increasing to 4 times the values of core A. Dashed lines showing average Hg concentration (62.4 ppb) and Hg/TOC (71.9 ppb/%) in shale from Grasby et al. (2019). The Hg/TOC profile in the Posidonienschiefer shows homogeneity, especially in core A.

the result of their more distal position relative to the paleo-shoreline (Figure 1; Dickson et al., 2022) with higher productivity and subdued siliciclastic input relative to the supply of organic matter.

With HI values around 600–750 and oxygen index (OI) values under 20 in core A (Figure 2), the Posidonienschiefer is a Type I/II kerogen (Figure S1 in Supporting Information S1, Espitalié et al., 1977) with a primary algal organic-matter-dominated maceral assemblage confirmed by organic geochemical and petrographic studies on these cores (Blumenberg et al., 2019; Celestino, 2019; Gorbanenko & Ligouis, 2014, 2015). These features are comparable to those in Toarcian sediments from other sections in the LSB and adjoining NW European basins (e.g., Littke et al., 1988, 1991; Schwark & Frimmel, 2004; French et al., 2014; Song et al., 2017). Analysis of the residual organic matter in cores B and C (Celestino, 2019) indicated that they also contained original organofacies that were comparable to those in core A; therefore, there is no evidence that depositional conditions favoring high productivity and preservation of organic matter in the Posidonienschiefer varied significantly across the basin.

Another factor resulting in the differences of TOC, and therefore organic-matter-related Hg, could be varied redox conditions in the paleogeographic locations of the three cores. Although the basin was generally characterized by anoxia and extensive euxinic depositional conditions, the presumed greater paleo-water depths of cores B and C and subtle variations in the intensity of euxinia and/or vertical extent of the euxinic water column may have resulted

Table 2

Average and Standard Deviation for Hg in Oils Derived From the Posidonienschiefer

Sample	Average Hg concentration (ppb)	*n* replicates
066.02	4.0 ± 1.9	5
066.05	2.6 ± 0.9	5
066.06	2.8 ± 2.1	5
066.09	5.2 ± 1.9	5
066.18	3.0 ± 2.9	5
066.21	2.5 ± 1.9	5
Mean	3.4 ± 1.1	

in higher TOC preservation efficiency and observed differences in TS and redox-sensitive and/or chalcophilic trace elements at the time of deposition. However, trace-element concentration profiles, iron-speciation data and organic petrography (Celestino, 2019; Dickson et al., 2020, 2022; Gorbanenko & Ligouis, 2014, 2015) demonstrate persistent anoxic/sulfidic conditions. Molybdenum concentration profiles for cores A and C (Figures 2 and 4) show remarkably similar trends up-section, implying that equivalent changes in depositional redox conditions through time affected both cores, despite the geographic distance between them. The similarity in Mo profiles between the cores and previous studies on the effects of maturation on concentrations and stable isotopes of Mo, Cd, U, and Zn in cores A and C (core B was not analyzed for Mo) found no evidence for significant differences in depositional redox conditions (Dickson et al., 2020, 2022). Hence, it is unlikely that redox conditions favoring preservation of the biomass varied significantly between the three core locations and within each Posidonienschiefer section, at least not to the extent that it could have appreciably influenced Hg deposition (Celestino, 2019; Dickson et al., 2020, 2022; Frieling et al., 2023; Gorbanenko & Ligouis, 2014, 2015).

The clay content differences between cores A, B, and C could be a possible alternative explanation related to Hg loading difference as well as TOC and TS. While clay is another commonly invoked Hg host phase (Shen et al., 2020), its importance as an Hg host phase seems limited to organic- and sulfur-lean sediments (e.g., Shen, Yu, et al., 2019). The higher original TOC in Cores B and C suggest that the organic-matter at these localities was less diluted, indicating that these depositional settings may have received less detrital matter, not more. Collectively, differences in clay content appear an unlikely explanation for causing any primary differences in Hg loading.

5.2. Carrier-Phase Depletion

It is generally accepted that Hg is hosted in both organic matter and sulfide minerals in organic-rich sedimentary rocks such as the Posidonienschiefer (e.g., Frieling et al., 2023; Grasby et al., 2017; Them et al., 2019). Nonetheless, the weak relationships between Hg concentrations and TOC or TS exhibited in the Posidonienschiefer sections may be a function of variable amounts of Hg being hosted in these two phases. Both elevated TOC and TS values are typical in sediments rich in labile organic matter, which may also contain substantial amounts of Hg. As discussed previously, labile organic matter can undergo transformation as a result of thermal stress (burial) and form mobile hydrocarbon and non-hydrocarbon phases that can be expelled from the sedimentary section where they are formed, resulting in an overall decrease in the amount of original TOC and consequent rock-mass loss (Dembicki, 2022; Lewan et al., 1979; Raiswell & Berner, 1987; Tissot & Welte, 1984). Although it is difficult to know precisely how much of the original organic-carbon of the Posidonienschiefer sediments in our study has been lost during maturation, using the reconstruction method of Jarvie (2012), we estimate that up to 50% of the original TOC in cores B and C may have been reduced as a result of kerogen conversion and hydrocarbon expulsion. Consequently, loss of organic carbon may have resulted in a significant (relative) enrichment in trace elements if these were retained in the host rock and not removed in a mobile fluid phase.

Such significant loss of TOC as a result of thermal maturation would result in proxies such as Hg/TOC shifting to higher ratios in mature and post-mature OM-rich rocks (Figures 5 and 6) compared to their immature equivalents if Hg were not significantly remobilized and expelled. Previous studies on these cores demonstrated that this process has also affected the concentrations of Cd, Zn, Mo, and U, which increased by as much as ∼10% (Cd), ∼20% (Zn), ∼45% (Mo), and, although more uncertain, 185% (U) from core A to core C (Dickson et al., 2022) (see Table 1). In addition to TOC loss, the expulsion of water from the dehydration of clays during burial and maturation also would have contributed to the loss of rock-mass (Peters & Cassa, 1994). The combination of TOC loss and host-rock mass loss from inorganic compounds would potentially result in a bias in both measured Hg and normalized Hg relative to the original signal stored in the rock record. As an example of this pitfall, one might infer a higher (>2 times) original Hg mass accumulation rate in cores B and C compared with core A if one did not take the thermal maturity level of each core into account, especially since the thicknesses of the Posidonienschiefer sections do not vary significantly.

5.3. Mobilization and Redeposition of Hg

The magnitude of change in Hg concentration compared to previously determined TOC loss (Dickson et al., 2020) shows that the increase in Hg can be partially explained by mass loss during catagenesis if Hg is considered nearly immobile. However, the notion that Hg is immobile during maturation appears at odds with previous findings

from maturation experiments (Chen et al., 2022; Liu et al., 2022), and data from metamorphic aureoles around igneous intrusions (Svensen et al., 2023) that showed progressive Hg loss with heating. Such distinct differences in Hg mobility between our naturally matured materials and previous studies (e.g., Chen et al., 2022; Liu et al., 2022; Svensen et al., 2023) might be explained by the fact (a) that our cores were deeply buried shale units with very limited permeability and (b) that Hg in the LSB does not seem to partition strongly into evolved fluids (Table 2). The oil contains ≤5 ppb Hg compared to the 50–150 ppb sedimentary Hg concentrations found in core A, supporting very limited partitioning. Compacted low-permeability shale units might have behaved more akin to a closed-system, whereby Hg released from its original host might have been re-sequestered by other phases over time. The effective mobility of Hg might have been further limited by the relatively low geological maximum temperatures (70–260°C) experienced by our material and the abundance of scavenging ligands (OM, sulfur), that might have permitted re-capture in pyrite, as HgS or as secondary Hg-OM complexes.

In addition to the constant-sum effects and speculative release–recapture in a closed system, as discussed above, other processes could also have played a role in elevating Hg concentrations in the mature cores. Such processes could include, for example, internal (lateral or, more unlikely, vertical) redistribution of Hg as a fluid or gas phase in the sediment column or capture of externally sourced Hg within the Posidonienschiefer. Even if net Hg mobility in these sedimentary strata was effectively zero, some degree of Hg release from its initial host-phase was expected during maturation. For example, the burial temperatures experienced by cores B and C (as much as 200 and 260°C, respectively) would have allowed (partial) release of Hg from common known sedimentary host phases such as OM and pyrite (Reis et al., 2012, 2015; Rumayor et al., 2013; Saniewska & Bełdowska, 2017). Mercury concentrations in core A are approximately stable within the Posidonienschiefer, whereas a distinct up-section increase is observed in cores B and C (Figure 6). While this chemostratigraphic pattern might be explained by Hg migration and (partial) re-capture in cores B and C, such a process is difficult to envisage in lithologies such as the Posidonienschiefer that have extremely low matrix porosity and permeability, especially after burial to depths of ~5,600 m (Bruns et al., 2013). Furthermore, the likelihood of 2 cores (B and C), which are separated by 10s of kilometers, resulting in similar Hg profiles after such a proposed redistribution seems very low.

5.4. Redistribution and Mobilization of Hg by Fractures and Veins

The maturation of organic matter and heating of sediments ultimately can lead to fluid overpressures and fracturing of low-porosity/permeability rocks (see Hooker et al., 2020 and references therein). For example, according to Meissner (1978), the catagenesis of solid kerogen into liquid hydrocarbons, gas, refractory carbon (e.g., graphite), and other by-products can increase local fluid pressures and result in hydraulic fracturing of the host lithology, and in the formation of veins (e.g., Lash & Engelder, 2005; Mandl & Harkness, 1987). Shale layers in highly mature to post-mature cores B and C contain abundant layer-parallel and oblique veins, mostly filled by calcite cement, with traces of pyrite crystals (Hooker et al., 2020). These oblique and bedding-parallel fractures containing so-called "beef" calcite may have played an important role in the primary migration of petroleum fluids within and from the Posidonienschiefer (Leythaeuser et al., 1988). These calcite veins in the mature cores also demonstrate that fluid passed through the stratigraphy at some point in the basin history and could have been the means of transport for a volatile or dissolved Hg phase, either during thermal maturation or afterward. However, Hooker et al. (2020) indicated that the potential for vertical migration of fluids through the fractures that are filled with calcite is low, as well as the postulated porosity and permeability within the fracture fill itself. Although we cannot indicate whether finer or larger scale fractures in the cores themselves or outside the core intervals have indeed played a role in redistributing Hg, the observation of diverging up-section Hg trends within some of the highly fractured intervals warrants caution.

5.5. Summary of Controls on Hg Concentrations in Cores A, B, and C

From the above discussions, we compiled a summary table of known syn- and post-sedimentary processes that might have influenced sedimentary Hg concentration in cores A, B, and C (Table 3). For these high-productivity anoxic conditions, Hg burial is effectively limited to the Hg supply from atmospheric and riverine sources (Fendley et al., 2024; Frieling et al., 2023; Schuster et al., 2018). The Hg supply limitation during deposition is also supported by the correlation, albeit weak, between Hg and Mo concentrations (Figure S4 in Supporting Information S1, Bian et al., 2024). When the Hg supply is limiting, Hg concentrations can no longer increase at the same rate as TOC, expressed as decreasing Hg/TOC with increasing TOC, for example, seen in the Hg/TOC between the Lias Delta and Posidonienschiefer in core A (4-fold increase in TOC concentration but only 2-fold

Table 3
Summary of All Processes Involved in Sedimentary Hg Concentrations in Cores A, B, and C in This Study

Time	Process	Difference between cores (core A, B to C)	Range of possible changes	Data
Syn-deposition	Hg in atmosphere (atmospheric deposition)	None expected		
	Hg from terrestrial material (land-derived OM)	Reduced in core B and C because of distance from paleoshoreline	Unknown	Zimmermann et al. (2018)
	Hg binding with marine organic-matter (algae in shallow marine environment)	Higher in core B and C because of higher TOC content	Max. ~200%	Frieling et al. (2023) and Fendley et al. (2024)
	Redox in water column and sediment	None expected		Dickson et al. (2020)
Post-deposition	Hydrocarbon generation/organic-matter loss	Core A: none, Core B and C: maximum organic mass loss ~50%		Hooker et al. (2020)
	Non organic-matter mass loss (dehydration)	Core A: none, Core B and C: ~5%–10%		Peters and Cassa (1994)
	Fracturing and fluid migration through fractures	Unknown		
	Hydrocarbon migration	None expected		This study (Hg in oil)
Observed	Catagenesis (oil window and gas window)	Increase from core A to B	~200%	This study
Result	Metagenesis (dry gas zone)	Increase from core B to C	10%	

increase in Hg, Figure 2). In order to explain the observed differences (Figure 5), the local Hg supply to cores B and C would have needed to be approximately twice as high as for core A. All three cores were in the same latitudinal band with similar rainfall patterns and rates of wet and dry Hg deposition (e.g., Jiskra et al., 2021); therefore, no major differences are expected between the cores in terms of the atmospheric Hg supply. Riverine Hg supply could have been important locally, but because of the more distal position of cores B and C relative to the paleoshoreline (cf. Zimmermann et al., 2018; Figure 1), this would likely have reduced the supply to B and C relative to A, resulting in a lower, not higher, total Hg supply for more distal parts of the basin. Thus, the increase in Hg concentration or changes in stratigraphic trends cannot be simply explained by differences in starting concentrations. This observation suggests that other, perhaps unlikely, maturation-related effects such as redistribution via fractures and veins may have to be considered.

5.6. Implications for the Use of the Hg Proxy in Mature Sediments

The Hg concentration of an average clastic sedimentary rock is 62.4 ppb according to the compilation in Grasby et al. (2019), and Hg/TOC values from the global inventory from the same study average around 71.9 ppb/%. Mercury concentrations in the Posidonienschiefer sections of much of core A and all of cores B and C are above the reported global averages (Figures 3 and 4) and are well within the range of anomalous "Hg spikes" in the geological record previously interpreted to result from LIP activity. However, because of the very high TOC, the TOC-normalized Hg data in all the cores in this study are significantly lower (Figures 2–4, 6, and Figure S3 in Supporting Information S1) than the range of recorded Hg/TOC values that are generally considered anomalous and interpreted as volcanic signatures.

In this study, we inferred a rise in Hg/TOC with maturation that is not easily explained by differences in starting Hg concentrations or by intra-basinal differences in depositional conditions. We consider this effect important for workers utilizing Hg/TOC ratios as a proxy for volcanism, as maturity-related changes may alter an interpretation where volcanic threshold values are used. Therefore, we consider it important to highlight the fact that maturation can result in a higher Hg/TOC signal, which could then be misinterpreted as consistent with enhanced volcanic loading. Very few published studies report the maturity level or exposure temperatures of their samples, but our observations show that a cautious approach when using samples that have been substantially matured is warranted. It is also worth noting that the effects of maturity become more important further back in the geological record, increasing the likelihood of the bias but nonetheless in many cases represent valuable targets for study.

Our findings further highlight that it is important to note that the use of normalized Hg as a volcanic proxy must be used with caution as Hg does not linearly scale with TOC due to a variety of (syn-)depositional processes (e.g., Fendley et al., 2024; Frieling et al., 2023, 2024; Grasby et al., 2019; Schuster et al., 2018). In addition, we must consider similar processes acting on relatively low-TOC samples; maturation in such settings could easily lead to values that (far) exceed the Hg/TOC shale value. As previously discussed, the variability in the Hg and Hg/TOC and Hg/TS profiles between the three cores, and within the Posidonienschiefer section of each core is, at this stage, difficult to explain without invoking unlikely factors such as Hg migration through low-permeability shales. The loss of rock mass during thermal maturation, and variation in hydrocarbon production may explain some of the variance in TOC and Hg/TOC ratios. However, the changes in Hg concentrations within the Posidonienschiefer sections of each core are likely related to other processes that we do not fully understand as yet. Redistribution of Hg cannot be ruled out; however, the similarity in profiles of cores B and C, and the extremely low permeability of the current overall Posidonienschiefer lithology, make such a process difficult to envisage. Regardless of the exact mechanisms, the change in the pattern of Hg concentration, and Hg/TOC and Hg/TS ratios between the three cores (Figure 6) shows that thermal maturation can displace, introduce, or remove Hg "spikes" in the geological record.

Assessing the extent of signal alteration caused by thermal maturation is more challenging as it requires extremely detailed knowledge of the original depositional and paleoenvironmental conditions of the examined sequence. In the current study, we have the advantage of evidence from the three cores with comparable biomass input and preservation, persistent and comparable redox conditions and high sampling resolution to compare, in detail, the correlated sections. Despite possible minor differences in initial Hg concentrations, we infer a clear rise in Hg/TOC ratios (and potentially also Hg) with maturation that is important for the proxy to be used for assessing anomalous Hg concentrations in the sedimentary record. Regardless of the precise mechanisms involved, the increase in Hg/TOC from TOC loss alone implies that knowledge of the thermal maturation history of the material

becomes critical for the interpretation of Hg records when analyzing sediments that have undergone significant burial and exposure to different maximum temperatures.

For periods when all records are thermally mature, as would be progressively more likely with sediment deposited further back in time, systematic changes might occur to Hg and normalized Hg values. These changes might include potential Hg spiking through remobilization and recapture, concentration or other enrichment processes (as explored here) or, after extreme heating, Hg depletion via mobilization and escape (Chen et al., 2022; Liu et al., 2022). Together, these potential changes lead to much increased uncertainties in terms of estimating volcanic (Hg) emissions from thermally mature sedimentary successions, although despite these challenges, many still yield very important data and insights.

6. Conclusions

Understanding Hg behavior during the thermal maturation of sediments is important in terms of our broader knowledge of its global cycling. It also further highlights how the thermal history of sediments is a necessary consideration when looking for anomalous Hg enrichments with the intention to use Hg as a proxy for volcanism. We have studied three cores with different levels of thermal maturity from the Lower Toarcian Posidonienschiefer in the Lower Saxony Basin, Germany. In contrast with other studies that show progressive Hg loss with heating in the thermal aureoles of sill intrusions or in laboratory experiments, maturation here appears to be associated with higher Hg concentrations. Mercury concentrations recorded in mature core B and post-mature core C were +132% to +157% higher than in immature core A. The very low Hg concentrations (≤ 5 ppb) in Posidonienschiefer-derived oils compared to the immature sediments (50–150 ppb) support the conclusion that Hg did not effectively partition into hydrocarbons during maturation and may be considered nearly immobile under these circumstances. At the same time, thermal maturation and hydrocarbon generation-migration reduced the TOC concentration of the host rock by up to ∼50% at the high levels of maturity in Cores B and C. As a consequence, Hg/TOC ratios from those mature sediments are considerably inflated relative to the immature material. Nonetheless, the observed increase in Hg concentrations with maturation cannot be easily explained by TOC or host-rock mass loss alone.

In search of a mechanism that may have resulted in differences between the three cores, we therefore discuss a suite of syn-depositional processes (i.e., atmospheric Hg and riverine Hg supply, distance from paleoshoreline, and redox conditions) and post-depositional (i.e., maturation related) processes. None of the known syn-depositional or post-depositional processes can satisfactorily explain the Hg increase from core A to core B and C. As syn-depositional processes are unlikely to have resulted in all the observed differences between core A and core B and C, we speculate that, to some degree, the pronounced difference in the variability of stratigraphic signals of Hg between cores A and core B and C is related to maturation effects, including Hg redistribution. Although the precise mechanisms of Hg mobilization and re-sequestration remain elusive, the calcite- and pyrite-filled fractures and veins that occur in certain intervals of cores B and C may hint at Hg migration into specific stratigraphic levels during or after hydrocarbon mobilization. Regardless of the exact mechanisms of Hg enrichment, and inflation of Hg/TOC, our results show that thermal maturation effects mean that a cautious approach is warranted when using (post)mature and especially fractured sedimentary successions as an archive for far-field subaerial volcanic activity. Our data show that in a broader sense sediment maturation processes are complex in terms of their contributions to Hg cycling and behavior.

Data Availability Statement

All data generated and used to conduct this study can be found in Indraswari et al. (2024).

References

Abarghani, A., Gentzis, T., Liu, B., Khatibi, S., Bubach, B., & Ostadhassan, M. (2020). Preliminary investigation of the effects of thermal maturity on redox-sensitive trace metal concentration in the Bakken source rock, North Dakota. *American Chemical Society Omega*, 5(13), 7135–7148. https://doi.org/10.1021/acsomega.9b03467

Ardakani, O. H., Hlohowskyj, S. R., Chappaz, A., Sanei, H., Liseroudi, M. H., & Wood, J. M. (2020). Molybdenum speciation tracking hydrocarbon migration in fine-grained sedimentary rocks. *Geochimica et Cosmochimica Acta*, 283, 136–148. https://doi.org/10.1016/J.GCA.2020.06.006

Baldschun, R., Kockel, F., Best, G., Deneke, E., Frisch, U., Juergens, U., et al. (1996). Geotektonischer Atlas vonNW-Deutschland/Tectonic Atlas of NW Germany (scale 1:300,000). *Bundesanstalt für Geowissenschaften und Rohstoffe, Hannover*.

Behar, F., Beaumont, V., & DePenteado, B. H. L. (2001). Rock-Eval 6 technology: Performances and developments. *Oil and Gas Science and Technology*, 56(2), 111–134. https://doi.org/10.2516/ogst:2001013

Benoit, J. M., Mason, R. P., Gilmour, C. C., & Aiken, G. R. (2001). Constants for mercury binding by organic matter isolates from the Florida Everglades. *Geochimica et Cosmochimica Acta*, *65*(24), 4445–4451. https://doi.org/10.1016/S0016-7037(01)00742-6

Betz, D., Führer, F., Greiner, G., & Plein, E. (1987). Evolution of the lower Saxony Basin. *Tectonophysics*, *137*(1–4), 127–170. https://doi.org/10.1016/0040-1951(87)90319-2

Bian, L., Chappaz, A., Schovsbo, N. H., Nielsen, A. T., & Sanei, H. (2022). High mercury enrichments in sediments from the Baltic continent across the late Cambrian: Controls and implications. *Chemical Geology*, *599*, 120846. https://doi.org/10.1016/J.CHEMGEO.2022.120846

Bian, L., Chappaz, A., Wang, X., Amouroux, D., Schovsbo, N. H., Zheng, X., & Sanei, H. (2024). Improving mercury systematics with molybdenum and vanadium enrichments: New insights from the Cambrian-Ordovician boundary. *Geophysical Research Letters*, *51*(8), e2023GL107188. https://doi.org/10.1029/2023GL107188

Bin, C., Xiaoru, W., & Lee, F. S. C. (2001). Pyrolysis coupled with atomic absorption spectrometry for the determination of mercury in Chinese medicinal materials. *Analytica Chimica Acta*, *447*(1–2), 161–169. https://doi.org/10.1016/S0003-2670(01)01218-1

Blumenberg, M., Zink, K. G., Scheeder, G., Ostertag-Henning, C., & Erbacher, J. (2019). Biomarker paleo-reconstruction of the German Wealden (Berriasian, Early Cretaceous) in the Lower Saxony Basin (LSB). *International Journal of Earth Sciences*, *108*(1), 229–244. https://doi.org/10.1007/s00531-018-1651-5

Bohacs, K. M., Norton, I. O., Neal, J. E., & Gilbert, D. (2020). The accumulation of organic-matter-rich rocks within an earth system's framework: The integrated roles of plate tectonics, atmosphere, ocean, and biota through the Phanerozoic. In N. Scarselli, et al. (Eds.), *Regional geology and tectonics: Volume 1: Principles of geologic analysis* (pp. 721–744). Elsevier. https://doi.org/10.1016/B978-0-444-64134-2.00023-7

Brink, H. J., Dürschner, H., & Trappe, H. (1992). Some aspects of the late and post-Variscan development of the Northwestern German Basin. *Tectonophysics*, *207*(1–2), 65–95. https://doi.org/10.1016/0040-1951(92)90472-I

Bruns, B., di Primio, R., Berner, U., & Littke, R. (2013). Petroleum system evolution in the inverted Lower Saxony Basin, northwest Germany: A 3D basin modeling study. *Geofluids*, *13*(2), 246–271. https://doi.org/10.1111/gfl.12016

Bryndzia, L. T., Burgess, J. M., & Bourdet, J. (2023). Predicting the solubility of mercury in hydrocarbons. *SPE Journal*, *28*(02), 859–875. https://doi.org/10.2118/212271-PA

Celestino, R. (2019). *Environmental change and carbon cycling during the Early Jurassic: A multi-proxy study on the Posidonienschiefer of NW Germany, (Doctoral dissertation).* University of Exeter. Retrieved from http://hdl.handle.net/10871/36576

Celestino, R., Ruhl, M., Dickson, A. J., Idiz, E., Jenkyns, H. C., Leng, M. J., et al. (n.d.). Protracted carbon burial following the Early Jurassic Toarcian oceanic anoxic event (Posidonia Shale, Lower Saxony Basin, Germany). *Submitted to International Journal of Earth Sciences*. (*Submitted*).

Chappaz, A., Lyons, T. W., Gregory, D. D., Reinhard, C. T., Gill, B. C., Li, C., & Large, R. R. (2014). Does pyrite act as an important host for molybdenum in modern and ancient euxinic sediments? *Geochimica et Cosmochimica Acta*, *126*, 112–122. https://doi.org/10.1016/j.gca.2013.10.028

Charbonnier, G., & Föllmi, K. B. (2017). Mercury enrichments in lower Aptian sediments support the link between Ontong Java large igneous province activity and oceanic anoxic episode 1a. *Geology*, *45*(1), 63–66. https://doi.org/10.1130/G38207.1

Chen, D., Ren, D., Deng, C., Tian, Z., & Yin, R. (2022). Mercury loss and isotope fractionation during high-pressure and high-temperature processing of sediments: Implication for the behaviors of mercury during metamorphism. *Geochimica et Cosmochimica Acta*, *334*, 231–240. https://doi.org/10.1016/J.GCA.2022.08.010

Dahl, T. W., Chappaz, A., Hoek, J., McKenzie, C. J., Svane, S., & Canfield, D. E. (2017). Evidence of molybdenum association with particulate organic matter under sulfidic conditions. *Geobiology*, *15*(2), 311–323. https://doi.org/10.1111/gbi.12220

Dal Corso, J., Mills, B. J. W., Chu, D., Newton, R. J., Mather, T. A., Shu, W., et al. (2020). Permo–Triassic boundary carbon and mercury cycling linked to terrestrial ecosystem collapse. *Nature Communications*, *11*(1), 2962. https://doi.org/10.1038/s41467-020-16725-4

Dembicki, H. (2022). *Practical petroleum geochemistry for exploration and production.* Elsevier. https://doi.org/10.1016/C2021-0-01572-8

Dickson, A. J., Idiz, E., Porcelli, D., Murphy, M. J., Celestino, R., Jenkyns, H. C., et al. (2022). No effect of thermal maturity on the Mo, U, Cd, and Zn isotope compositions of Lower Jurassic organic-rich sediments. *Geology*, *50*(5), 598–602. https://doi.org/10.1130/g49724.1

Dickson, A. J., Idiz, E., Porcelli, D., & van den Boorn, S. H. J. M. (2020). The influence of thermal maturity on the stable isotope compositions and concentrations of molybdenum, zinc and cadmium in organic-rich marine mudrocks. *Geochimica et Cosmochimica Acta*, *287*, 205–220. https://doi.org/10.1016/j.gca.2019.11.001

Espitalié, J., Laporte, J. L., Madec, M., Marquis, F., Leplat, P., Paulet, J., & Boutefeu, A. (1977). Méthode rapide de caractérisation des roches mètres, de leur potentiel pétrolier et de leur degré d'évolution. *Revue de l'Institut Français Du Pétrole*, *32*(1), 23–42. https://doi.org/10.2516/ogst:1977002

Evenick, J. C. (2021). Examining the relationship between Tmax and vitrinite reflectance: An empirical comparison between thermal maturity indicators. *Journal of Natural Gas Science and Engineering*, *91*, 103946. https://doi.org/10.1016/J.JNGSE.2021.103946

Fantasia, A., Föllmi, K. B., Adatte, T., Bernárdez, E., Spangenberg, J. E., & Mattioli, E. (2018). The Toarcian oceanic anoxic event in southwestern Gondwana: An example from the Andean Basin, northern Chile. *Journal of the Geological Society*, *175*(6), 883–902. https://doi.org/10.1144/jgs2018-008

Fendley, I. M., Frieling, J., Mather, T. A., Ruhl, M., Hesselbo, S. P., & Jenkyns, H. C. (2024). Early Jurassic large igneous province carbon emissions constrained by sedimentary mercury. *Nature Geoscience*, *17*(3), 241–248. https://doi.org/10.1038/s41561-024-01378-5

Filby, R. H. (1994). Origin and nature of trace element species in crude oils, bitumens and kerogens: Implications for correlation and other geochemical studies. In J. Parnell (Ed.), *Geofluids: Origin, migration and evolution of fluids in sedimentary basins. Geological society, London, special publications* (Vol. 78(1), pp. 203–219). https://doi.org/10.1144/GSL.SP.1994.078.01.15

Fitzgerald, W. F., & Lamborg, C. H. (2014). Geochemistry of Mercury in the environment. In H. D. Holland & K. K. Turekian (Eds.), *Treatise on geochemistry* (2nd ed., Vol. 11, pp. 91–129). Elsevier Inc. https://doi.org/10.1016/B978-0-08-095975-7.00904-9

French, K. L., Sepúlveda, J., Trabucho-Alexandre, J., Gröcke, D. R., & Summons, R. E. (2014). Organic geochemistry of the early Toarcian oceanic anoxic event in Hawsker Bottoms, Yorkshire, England. *Earth and Planetary Science Letters*, *390*, 116–127. https://doi.org/10.1016/j.epsl.2013.12.033

Frieling, J., Fendley, I. M., Nawaz, M. A., & Mather, T. A. (2024). Assessment of Hg speciation changes in the sedimentary rock record from thermal desorption characteristics. *Geochemistry, Geophysics, Geosystems*, *25*(4), e2024GC011502. https://doi.org/10.1029/2024GC011502

Frieling, J., Mather, T. A., März, C., Jenkyns, H. C., Hennekam, R., Reichart, G.-J., et al. (2023). Effects of redox variability and early diagenesis on marine sedimentary Hg records. *Geochimica et Cosmochimica Acta*, *351*, 78–95. https://doi.org/10.1016/J.GCA.2023.04.015

Gluyas, J. G., & Swarbrick, R. E. (2021). *Petroleum geoscience.* John Wiley & Sons.

Gorbanenko, O., & Ligouis, B. (2014). Changes in optical properties of liptinite macerals from early mature to post mature stage in Posidonia Shale (Lower Toarcian, NW Germany). *International Journal of Coal Geology*, *133*, 47–59. https://doi.org/10.1016/j.coal.2014.09.007

Gorbanenko, O., & Ligouis, B. (2015). Variations of organo-mineral microfacies of Posidonia Shale from the Lower Saxony Basin and the West Netherlands Basin: Application to paleoenvironmental reconstruction. *International Journal of Coal Geology*, *152*, 78–99. https://doi.org/10.1016/j.coal.2015.09.011

Grasby, S. E., Shen, W., Yin, R., Gleason, J. D., Blum, J. D., Lepak, R. F., et al. (2017). Isotopic signatures of mercury contamination in latest Permian oceans. *Geology*, *45*(1), 55–58. https://doi.org/10.1130/G38487.1

Grasby, S. E., Them, T. R., Chen, Z., Yin, R., & Ardakani, O. H. (2019). Mercury as a proxy for volcanic emissions in the geologic record. *Earth-Science Reviews*, *196*(March), 102880. https://doi.org/10.1016/j.earscirev.2019.102880

Hooker, J. N., Ruhl, M., Dickson, A. J., Hansen, L. N., Idiz, E., Hesselbo, S. P., & Cartwright, J. (2020). Shale anisotropy and natural hydraulic fracture propagation: An example from the Jurassic (Toarcian) Posidonienschiefer, Germany. *Journal of Geophysical Research: Solid Earth*, *125*(3), e2019JB018442. https://doi.org/10.1029/2019JB018442

Indraswari, A., Frieling, J., Mather, T. A., Dickson, A. J., Jenkyns, H. C., & Idiz, E. (2024). Data supplement to "Investigating the behavior of sedimentary mercury (Hg) during burial-related thermal maturation" [Dataset]. *Figshare*. https://doi.org/10.6084/m9.figshare.25965901

Jarvie, D. M. (2012). Shale resource systems for oil and gas: Part1—Shale-gas resource systems. In J. A. Breyer (Ed.), *Shale reservoirs—Giant resources for the 21st century: American association of petroleum geologists memoir* (Vol. 97, pp. 69–87). The American Association of Petroleum Geologists. https://doi.org/10.1306/13321446m973489

Jenkyns, H. C. (1985). The early Toarcian and Cenomanian-Turonian anoxic events in Europe: Comparisons and contrasts. *Geologische Rundschau*, *74*(3), 505–518. https://doi.org/10.1007/BF01821208

Jenkyns, H. C. (1988). The early Toarcian (Jurassic) anoxic event; stratigraphic, sedimentary and geochemical evidence. *American Journal of Science*, *288*(2), 101–151. https://doi.org/10.2475/ajs.288.2.101

Jenkyns, H. C. (2010). Geochemistry of oceanic anoxic events. *Geochemistry, Geophysics, Geosystems*, *11*(3), Q03004. https://doi.org/10.1029/2009GC002788

Jiskra, M., Heimbürger-Boavida, L.-E., Desgranges, M.-M., Petrova, M. V., Dufour, A., Ferreira-Araujo, B. et al. (2021). Mercury stable isotopes constrain atmospheric sources to the ocean. *Nature*, *597*(7878), 678–682. https://doi.org/10.1038/s41586-021-03859-8

Kockel, F., Wehner, H., & Gerling, P. (1994). Petroleum systems of the Lower Saxony Basin, Germany. In L. B. Magoon & W. G. Dow (Eds.), *The petroleum system—from source to trap, American association of petroleum geologists memoir* (Vol. 60, pp. 573–586). The American Association of Petroleum Geologists. https://doi.org/10.1306/M60585C34

Lash, G. G., & Engelder, T. (2005). An analysis of horizontal microcracking during catagenesis: Example from the Catskill delta complex. *American Association of Petroleum Geologists Bulletin*, *89*(11), 1433–1449. https://doi.org/10.1306/05250504141

Lewan, M. D., & Maynard, J. (1982). Factors controlling enrichment of vanadium and nickel in the bitumen of organic sedimentary rocks. *Geochimica et Cosmochimica Acta*, *46*(12), 2547–2560. https://doi.org/10.1016/0016-7037(82)90377-5

Lewan, M. D., Winters, J. C., & Mcdonald, J. H. (1979). Generation of oil-like pyrolyzates from organic-rich shales. *Science*, *203*(4383), 897–899. http://www.jstor.org/stable/1747886

Leythaeuser, D., Littke, R., Radke, M., & Schaefer, R. G. (1988). Geochemical effects of petroleum migration and expulsion from Toarcian source rocks in the Hils syncline area, NW-Germany. *Organic Geochemistry*, *13*(1–3), 489–502. https://doi.org/10.1016/0146-6380(88)90070-8

Li, J., Han, Z., Yan, Q., Wang, S., & Ge, S. (2019). Distribution and genesis of mercury in natural gas of large coal derived gas fields in China. *Petroleum Exploration and Development*, *46*(3), 463–470. https://doi.org/10.1016/S1876-3804(19)60027-3

Li, X., Wang, Q., Zhang, W., & Yin, H. (2016). Contact metamorphism of shales intruded by a granite dike: Implications for shale gas preservation. *International Journal of Coal Geology*, *159*, 96–106. https://doi.org/10.1016/j.coal.2016.03.016

Littke, R., Baker, D. R., & Leythaeuser, D. (1988). Microscopic and sedimentologic evidence for the generation and migration of hydrocarbons in Toarcian source rocks of different maturities. *Organic Geochemistry*, *13*(1–3), 549–559. https://doi.org/10.1016/0146-6380(88)90075-7

Littke, R., Leythaeuser, D., Rullkötter, J., & Baker, D. R. (1991). Keys to the depositional history of the Posidonia Shale (Toarcian) in the Hils Syncline, northern Germany. In R. V. Tyson & T. H. Pearson (Eds.), *Modern and ancient continental shelf anoxia. Geological society special publication* (Vol. 58(1), pp. 311–333). https://doi.org/10.1144/GSL.SP.1991.058.01.20

Liu, Q. (2013). Mercury concentration in natural gas and its distribution in the Tarim Basin. *Science China Earth Sciences*, *56*(8), 1371–1379. https://doi.org/10.1007/s11430-013-4609-2

Liu, Q., Peng, W., Li, J., & Wu, X. (2020). Source and distribution of mercury in natural gas of major petroliferous basins in China. *Science China Earth Sciences*, *63*(5), 643–648. https://doi.org/10.1007/s11430-019-9596-6

Liu, Z., Tian, H., Yin, R., Chen, D., & Gai, H. (2022). Mercury loss and isotope fractionation during thermal maturation of organic-rich mudrocks. *Chemical Geology*, *612*, 121144. https://doi.org/10.1016/j.chemgeo.2022.121144

Mandl, G., & Harkness, R. M. (1987). Hydrocarbon migration by hydraulic fracturing. In M. E. Jones & R. M. F. Preston (Eds.), *Deformation of sediments and sedimentary rocks* (Vol. 29(1), pp. 39–53). *Geological society special publication*. https://doi.org/10.1144/GSL.SP.1987.029.01.04

Meissner, F. F. (1978). Petroleum geology of the Bakken formation Williston basin, North Dakota and Montana. In D. Estelle & R. Miller (Eds.), *Montana geological society: 24th annual conference: 1978 Williston basin symposium* (pp. 207–227). Montana Geological Society.

Montero-Serrano, J. C., Föllmi, K. B., Adatte, T., Spangenberg, J. E., Tribovillard, N., Fantasia, A., & Suan, G. (2015). Continental weathering and redox conditions during the early Toarcian Oceanic anoxic event in the northwestern Tethys: Insight from the Posidonia Shale section in the Swiss Jura Mountains. *Palaeogeography, Palaeoclimatology, Palaeoecology*, *429*, 83–99. https://doi.org/10.1016/J.PALAEO.2015.03.043

Mukherjee, A. B., Bhattacharya, P., Sarkar, A., & Zevenhoven, R. (2009). Mercury emissions from industrial sources in India and its effects in the environment. In R. Mason & N. Pirrone (Eds.), *Mercury fate and transport in the global atmosphere: Emissions, measurements and models* (pp. 81–112). Springer US. https://doi.org/10.1007/978-0-387-93958-2_4

Outridge, P. M., Sanei, H., Stern, G. A., Hamilton, P. B., & Goodarzi, F. (2007). Evidence for control of mercury accumulation rates in Canadian High Arctic Lake sediments by variations of aquatic primary productivity. *Environmental Science and Technology*, *41*(15), 5259–5265. https://doi.org/10.1021/es070408x

Percival, L. M. E., Bergquist, B. A., Mather, T. A., & Sanei, H. (2021). Sedimentary mercury enrichments as a tracer of large igneous province volcanism. In R. E. Ernst, A. J. Dickson, & A. Bekker (Eds.), *Large igneous provinces: A driver of global environmental and biotic changes, geophysical monograph series* (Vol. 255, pp. 247–262). American Geophysical Union and John Wiley and Sons, Inc. https://doi.org/10.1002/9781119507444.ch11

Percival, L. M. E., Jenkyns, H. C., Mather, T. A., Dickson, A. J., Batenburg, S. J., Ruhl, M., et al. (2018). Does large igneous province volcanism always perturb the mercury cycle? Comparing the records of Oceanic Anoxic Event 2 and the end-Cretaceous to other Mesozoic events. *American Journal of Science*, *318*(8), 799–860. https://doi.org/10.2475/08.2018.01

Percival, L. M. E., Witt, M. L. I., Mather, T. A., Hermoso, M., Jenkyns, H. C., Hesselbo, S. P., et al. (2015). Globally enhanced mercury deposition during the end-Pliensbachian extinction and Toarcian OAE: A link to the Karoo – Ferrar Large Igneous Province. *Earth and Planetary Science Letters*, *428*, 267–280. https://doi.org/10.1016/j.epsl.2015.06.064

Peters, K. E., & Cassa, M. R. (1994). Applied source rock geochemistry. In L. B. Magoon & W. G. Dow (Eds.), *The petroleum system—from source to trap, American association of petroleum geologists memoir* (Vol. 60, pp. 93–120). The American Association of Petroleum Geologists. https://doi.org/10.1306/M60585C5

Peters, K. E., Walters, C., & Moldowan, J. (2005). *The biomarker guide* (2nd ed.). Cambridge University Press. https://doi.org/10.1017/CBO9780511524868

Pyle, D. M., & Mather, T. A. (2003). The importance of volcanic emissions for the global atmospheric mercury cycle. *Atmospheric Environment*, *37*(36), 5115–5124. https://doi.org/10.1016/j.atmosenv.2003.07.011

Raiswell, R., & Berner, R. A. (1987). Organic carbon losses during burial and thermal maturation of normal marine shales. *Geology*, *15*(9), 853–856. https://doi.org/10.1130/0091-7613(1987)15<853:OCLDBA>2.0.CO;2

Reis, A. T., Coelho, J. P., Rodrigues, S. M., Rocha, R., Davidson, C. M., Duarte, A. C., & Pereira, E. (2012). Development and validation of a simple thermo-desorption technique for mercury speciation in soils and sediments. *Talanta*, *99*, 363–368. https://doi.org/10.1016/j.talanta.2012.05.065

Reis, A. T., Coelho, J. P., Rucandio, I., Davidson, C. M., Duarte, A. C., & Pereira, E. (2015). Thermo-desorption: A valid tool for mercury speciation in soils and sediments? *Geoderma*, *237–238*, 98–104. https://doi.org/10.1016/J.GEODERMA.2014.08.019

Röhl, H. J., Schmid-Röhl, A., Oschmann, W., Frimmel, A., & Schwark, L. (2001). The Posidonia Shale (Lower Toarcian) of SW-Germany: An oxygen-depleted ecosystem controlled by sea level and palaeoclimate. *Palaeogeography, Palaeoclimatology, Palaeoecology*, *165*(1–2), 27–52. https://doi.org/10.1016/S0031-0182(00)00152-8

Rullkötter, J., Leythaeuser, D., Horsfield, B., Littke, R., Mann, U., Müller, P. J., et al. (1988). Organic matter maturation under the influence of a deep intrusive heat source: A natural experiment for quantitation of hydrocarbon generation and expulsion from a petroleum source rock (Toarcian shale, northern Germany). *Organic Geochemistry*, *13*(4–6), 847–856. https://doi.org/10.1016/0146-6380(88)90237-9

Rumayor, M., Diaz-Somoano, M., Lopez-Anton, M. A., & Martinez-Tarazona, M. R. (2013). Mercury compounds characterization by thermal desorption. *Talanta*, *114*, 318–322. https://doi.org/10.1016/j.talanta.2013.05.059

Sanei, H., Grasby, S. E., & Beauchamp, B. (2012). Latest Permian mercury anomalies. *Geology*, *40*(1), 63–66. https://doi.org/10.1130/G32596.1

Saniewska, D., & Bełdowska, M. (2017). Mercury fractionation in soil and sediment samples using thermo-desorption method. *Talanta*, *168*, 152–161. https://doi.org/10.1016/j.talanta.2017.03.026

Schmid-Röhl, A., Röhl, H. J., Oschmann, W., Frimmel, A., & Schwark, L. (2002). Palaeoenvironmental reconstruction of Lower Toarcian epicontinental black shales (Posidonia Shale, SW Germany): Global versus regional control. *Geobios*, *35*(1), 13–20. https://doi.org/10.1016/S0016-6995(02)00005-0

Schuster, P. F., Schaefer, K. M., Aiken, G. R., Antweiler, R. C., Dewild, J. F., GryziecGusmeroli, J. D. A., et al. (2018). Permafrost stores a globally significant amount of mercury. *Geophysical Research Letters*, *45*(3), 1463–1471. https://doi.org/10.1002/2017GL075571

Schwark, L., & Frimmel, A. (2004). Chemostratigraphy of the Posidonia Black Shale, SW-Germany II. Assessment of extent and persistence of photic-zone anoxia using aryl isoprenoid distributions. *Chemical Geology*, *206*(3–4), 231–248. https://doi.org/10.1016/j.chemgeo.2003.12.008

Senglaub, Y., Littke, R., & Brix, M. R. (2006). Numerical modelling of burial and temperature history as an approach for an alternative interpretation of the Bramsche anomaly, Lower Saxony Basin. *International Journal of Earth Sciences*, *95*(2), 204–224. https://doi.org/10.1007/s00531-005-0033-y

Shen, J., Algeo, T. J., Chen, J., Planavsky, N. J., Feng, Q., Yu, J., & Liu, J. (2019). Mercury in marine Ordovician/Silurian boundary sections of South China is sulfide-hosted and non-volcanic in origin. *Earth and Planetary Science Letters*, *511*, 130–140. https://doi.org/10.1016/j.epsl.2019.01.028

Shen, J., Feng, Q., Algeo, T. J., Liu, J., Zhou, C., Wei, W., et al. (2020). Sedimentary host phases of mercury (Hg) and implications for use of Hg as a volcanic proxy. *Earth and Planetary Science Letters*, *543*, 116333. https://doi.org/10.1016/j.epsl.2020.116333

Shen, J., Yu, J., Chen, J., Algeo, T. J., Xu, G. Z., Feng, Q., et al. (2019). Mercury evidence of intense volcanic effects on land during the Permian-Triassic transition. *Geology*, *47*(12), 1117–1121. https://doi.org/10.1130/G46679.1

Song, J., Littke, R., & Weniger, P. (2017). Organic geochemistry of the Lower Toarcian Posidonia Shale in NW Europe. *Organic Geochemistry*, *106*, 76–92. https://doi.org/10.1016/j.orggeochem.2016.10.014

Stock, A., & Littke, R. (2016). Geochemical composition of oils from the Gifhorn Trough and Lower Saxony Basin in comparison to Posidonia Shale source rocks from the Hils Syncline Northern Germany. *German Journal of Gastroenterology*, *167*(2–3), 315–331. https://doi.org/10.1127/zdgg/2016/0058

Svensen, H. H., Jones, M. T., Percival, L. M. E., Grasby, S., & Mather, T. A. (2023). Release of mercury during contact metamorphism of shale: Implications for understanding the impacts of large igneous province volcanism. *Earth and Planetary Science Letters*, *619*, 118306. https://doi.org/10.1016/j.epsl.2023.118306

Them, T. R., Gill, B. C., Caruthers, A. H., Gröcke, D. R., Tulsky, E. T., Martindale, R. C., et al. (2017). High-resolution carbon isotope records of the Toarcian Oceanic anoxic event (Early Jurassic) from North America and implications for the global drivers of the Toarcian carbon cycle. *Earth and Planetary Science Letters*, *459*, 118–126. https://doi.org/10.1016/j.epsl.2016.11.021

Them, T. R., Jagoe, C. H., Caruthers, A. H., Gill, B. C., Grasby, S. E., Gröcke, D. R., et al. (2019). Terrestrial sources as the primary delivery mechanism of mercury to the oceans across the Toarcian oceanic anoxic event (Early Jurassic). *Earth and Planetary Science Letters*, *507*, 62–72. https://doi.org/10.1016/j.epsl.2018.11.029

Thibodeau, A. M., Ritterbush, K., Yager, J. A., West, A. J., Ibarra, Y., Bottjer, D. J., et al. (2016). Mercury anomalies and the timing of biotic recovery following the end-Triassic mass extinction. *Nature Communications*, *7*(1), 11147. https://doi.org/10.1038/ncomms11147

Tissot, B. P., & Welte, D. H. (1984). Sedimentary processes and the accumulation of organic matter. In B. P. Tissot & D. H. Welte (Eds.), *Petroleum formation and occurrence* (pp. 55–62). Springer-Verlag. https://doi.org/10.1007/978-3-642-96446-6_5

UN Environment. (2019). *Global mercury assessment 2018*. UN Environment Programme, Chemicals and Health Branch Geneva. Retrieved from https://www.unep.org/resources/publication/global-mercury-assessment-2018

Wallace, G. T. (1982). The association of copper, mercury and lead with surface-active organic matter in coastal seawater. *Marine Chemistry*, *11*(4), 379–394. https://doi.org/10.1016/0304-4203(82)90032-9

Wang, X., Cawood, P. A., Zhao, H., Zhao, L., Grasby, S. E., Chen, Z. Q., et al. (2018). Mercury anomalies across the end Permian mass extinction in South China from shallow and deep water depositional environments. *Earth and Planetary Science Letters*, *496*, 159–167. https://doi.org/10.1016/j.epsl.2018.05.044

Wilhelm, M., & Bloom, N. (2000). Mercury in petroleum. *Fuel Processing Technology*, *63*(1), 1–27. https://doi.org/10.1016/S0378-3820(99)00068-5

Wilhelm, S. M. (2001). Estimate of mercury emissions to the atmosphere from petroleum. *Environmental Science and Technology*, *35*(24), 4704–4710. https://doi.org/10.1021/es001804h

Zettlitzer, M., Scholer, H. F., Eiden, R., & Falter, R. (1997). Determination of elemental, inorganic and organic Mercury in North German Gas condensates and formation brines. In *International symposium on oilfield chemistry, February 18–21, 1997, Houston, Texas*. https://doi.org/10.2118/37260-MS

Zimmermann, J., Franz, M., Schaller, A., & Wolfgramm, M. (2018). The Toarcian–Bajocian deltaic system in the North German Basin: Subsurface mapping of ancient deltas-morphology, evolution and controls. *Sedimentology*, *65*(3), 897–930. https://doi.org/10.1111/sed.12410